Analysis of edge fluctuations on the CASTOR tokamak

J. Stöckel, V. Dhyani[1], J.Holakovský[2], L. Kryška, J. Petržílka[3], V. Svoboda[4], F. Žáček
Institute of Plasma Physics, Czech Acad. Sci., Prague, Czech Republic

Introduction

Edge fluctuations play a dominant role in the anomalous particle losses from tokamak plasma. In particular, recent lower hybrid current drive (LHCD) experiments in low density plasmas on ASDEX [1] and CASTOR [2] tokamaks demonstrated an improvement of the particle confinement at moderate lower hybrid powers, which is linked closedly to a reduction of edge electrostatic fluctuations. The mechanism of the fluctuation reduction is discussed elsewhere [3]. This contribution is devoted to a more detail characterization of electrostatic and magnetic fluctuations in this regime.

CASTOR tokamak

Experiments were carried out on the CASTOR tokamak ($R = 0.4\ m, a = 0.085\ m$) at $B_t = 1\ T$, $I_p = 12\ kA$ and densities $\bar{n}_e = 2{-}6{\cdot}10^{18}\ m^{-3}$. For LHCD, the lower hybrid wave ($f = 1.25\ GHz, P_{LH} \leq 40\ kW$) was launched into the plasma via the three-waveguide multijunction grill [2] during the quasistationary phase of discharge. A brief survey of fluctuation measurements follows:

A) Oscillatory technique for T_e – measurements (OH)

A sinusoidal voltage $V = V_0 \sin \omega t$ is applied to a Langmuir probe as shown in Fig. 1. The floating potential of the probe drops due to the rectification of electron current as [4]:

$$\Delta V_{fl} = T_e \ln \mathcal{J}(V_0/T_e) \qquad (\simeq V_0^2/4T_e \quad \text{for} \quad T_e > V_0)$$

where $\mathcal{J}(V_0/T_e)$ is the modified Bessel function and $T_e \equiv kT_e/e$.

Results of measurements are shown in Fig. 2. The frequency of sinusoidal modulation is 0.5 MHz, the amplitude V_0 is gated to determine the drop ΔV_{fl} by means of a single tip (the top trace). The middle trace shows the raw signal. The marks indicate the interpolated values of the signal with and without modulation. The resulting temperature (the bottom trace) is compared with evolution of T_e measured by a triple probe located in the vicinity of the oscillatory tip. The satisfactory agreement suggests that the oscillatory technique can be used if strictly local measurements of the electron temperature are needed.

Further, we test this technique to determine the T_e- fluctuations. For this, three tips spaced poloidally by 2.5 mm were used, the sinusoidal voltage being applied to the central one. The floating potential in this spatial point, necessary for determination of ΔV_{fl}, was estimated by the interpolation of data from the neighbouring floating tips. The relative level of temperature fluctuations $\tilde{T}_e/T_e \doteq 0.12$ obtained seems to be quite reasonable.

B) Mapping of the floating potential (OH)

The linear array of tips spaced poloidally by 2.5mm was used to investigate poloidal asymmetries in the plasma edge and to determine the correlation length of electrostatic fluctuations. The probe array was movable on a shot to shot basis.

[1]Cultural Exchange Programme, India
[2]Institute of Physics, Czech Acad. Sci., Prague
[3]Math.- Phys. Faculty, Charles University, Prague
[4]Faculty of Nuclear Sciences and Physical Engineering, Czech Tech. Univ., Prague

Fig. 3 depicts evolution of the raw signals of floating potential (sampled by $1\mu s$) from eight adjacent tips in a 2D plot for two radial positions of the array. It is evident that the perturbations propagate mostly from the tip No. 8 to the tip No.1 (which coresponds to the direction of electron diamagnetic drift) when the probe is within the limiter radius ($a > r = 83mm$), while a reverse tendency is apparent for a more outward position of the array.

The propagation velocity in poloidal direction was deduced by the correlation analysis. Fig. 4 manifests the variation of the form of crosscorrelation function with the radial position of the probe (2D plot, two tips are spaced by 5 mm). The direction of poloidal velocity corresponds to the cross-field drift velocity $(\vec{E}_r \times \vec{B}_t)/B_t^2$. The velocity shear layer is located close to the region with $E_r \sim -\partial V_{fl}/\partial r = 0$ (see Fig. 5).

C) Correlation analysis of magnetic fluctuations (OH + LHCD)

Poloidal magnetic fluctuations are monitored by two magnetic probes fixed inside the liner, their poloidal distance is 37 mm. The correlation functions of the probe signals are shown in Fig. 7. Typically, the cross-correlation function has two maxima. The maximum with a higher correlation ($C_{ij} > 0.5$) characterizes magnetic fluctuations propagating in the electron diamagnetic drift direction. We suppose, in concordance with Langmuir probe measurements, that these fluctuations have the origin within the plasma ($r < a$). The fluctuations related to the positive time delay of cross-correlation function are interpreted as a consequence of perturbations located within the scrape-off layer and propagating in the ion dimagnetic drift direction.

The time delay of both the maxima decreases with LHCD, which indicates an enhancement of the poloidal velocity of magnetic fluctuations which is also manifested by narrowing of the autocorrelation function. The similar effects are observed for the electrostatic fluctuations as well [6].

D) Dimensional and correlation analysis of density fluctuations (OH+LHCD)

To characterize whether the fluctuations are stochastic or chaotic (with less degrees of freedom than a noise), we calculated the correlation dimension of density fluctuations using the Grassberger-Procaccia algorithm [5]. The ion saturation current of a Langmuir probe is sampled by $0.2\mu s$ and 4096 samples (denoted as x_i) can be stored per a shot.

The dimensional analysis consists in construction of n-dimensional vectors from the data, n is the embedding dimension:

$$\vec{r_i} = (x_i + x_{i+d} + x_{i+2d} + ... + x_{i+(n-1)d}) \qquad i = 1, 2, ..., 4096 - (n-1)d \quad .$$

The correlation between the individual vector components should be negligible, therefore, we take the delay d as the autocorrelation time τ, defined as a halfwidth of autocorrelation function. Result for OH and LHCD regimes are summarized in Fig. 6.

Fig. 6a compares the dimensionality in LHCD and OH regimes for the probe position close to the limiter radius. The dimensionality in both the regimes seems to be lower than the same quantity for the computer-generated Gaussian noise in the all embedding dimensions. Further, the LHCD data are closer to the noise than the OH ones. This suggests that the density fluctuations in the LHCD regime (with reduced fluctuations and improved confinement [2]) are more stochastic. Our limited set of data do not allow to reach the saturation of dimensionality (even if exists).

Further, we compute the radial profiles of dimensionality (in the embedding dimension

n=4 only), see Fig. 6b. It is interesting to note that their form is linked to the radial profile of autocorrelation time, see Fig. 6c. When the dimensionality in LHCD is higher than in the OH regime, the autocorrelation time is lower and *vice versa*. Therefore, we investigated the relation between these two quantities in more detail. Fig. 6d is a plot of the dimensionality of data from a shot versus the time delay d. Note that the typical autocorrelation time for our data is $2-7\mu s$ (d = 10-35 samples). In this range of d, the dimensionality is practically independent on the delay and the difference between LHCD and OH regimes remains nearly constant. It seems, therefore, that the observed effects are not caused by an improper choice of the delay.

Acknowledgement: The work was performed under the Grant of Czech Acad. Sci. No. 14310 and supported by the IAEA Contract No. 6702/R1/RB

References

[1] Stöckel J, Söldner F.X et al.: Rep. IPP 1/268, Garching, 1992
[2] Stöckel J. et al.: IAEA TCM on Research Using Small Tokamaks, Würzburg, 1992
[3] Voitsekhovich I.A et al.: this Conference
[4] Ivanov R.S. et al.: Textor Rep. Jul-2432, January 1991
[7] Grassberger P., Procaccia I.: Phys. Rev. Lett.,50, 1983, 346

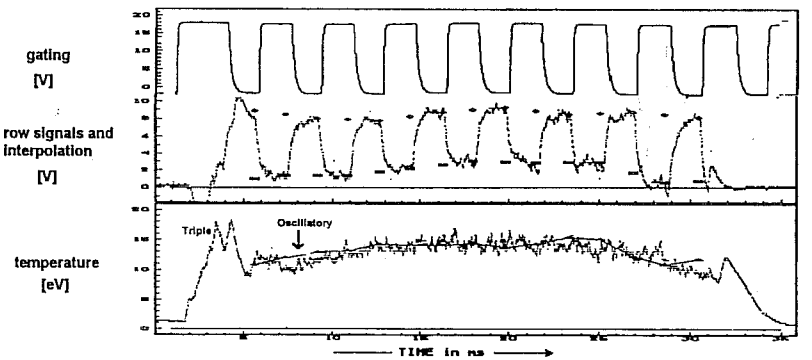

Fig.2. Temporal evolution of signals of the oscillatory probe

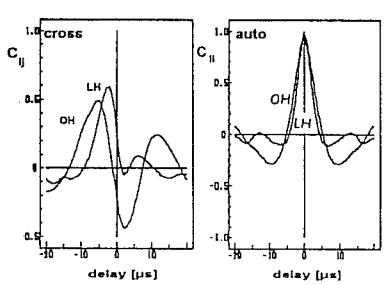

Fig.7 Correlations of magnetic fluctuations

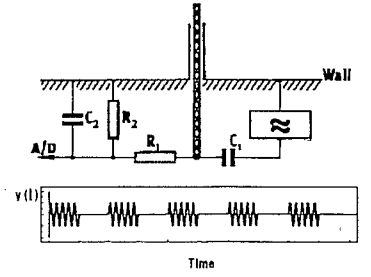

Fig.1. Arrangement of the oscillatory probe

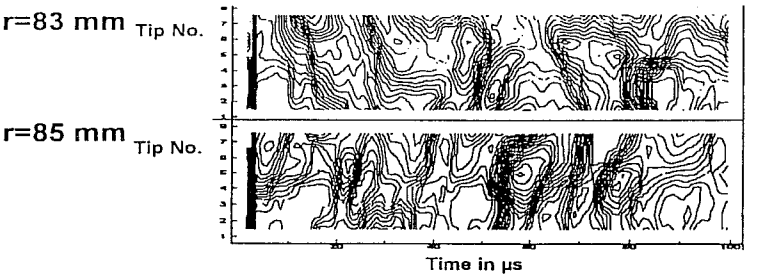

Fig.3. Evolution of floating potential monitored by 8 tips (2D plot)

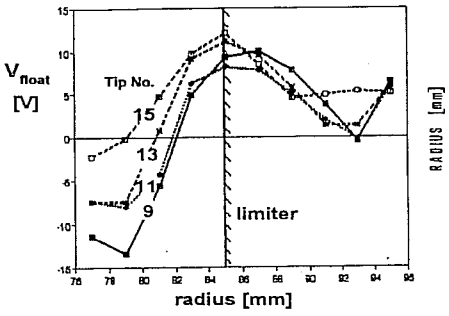

Fig.4. Radial profile of V_{float}

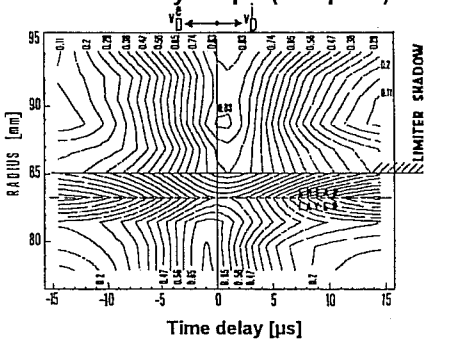

Fig.5. Crosscorrelation of tips 1-3

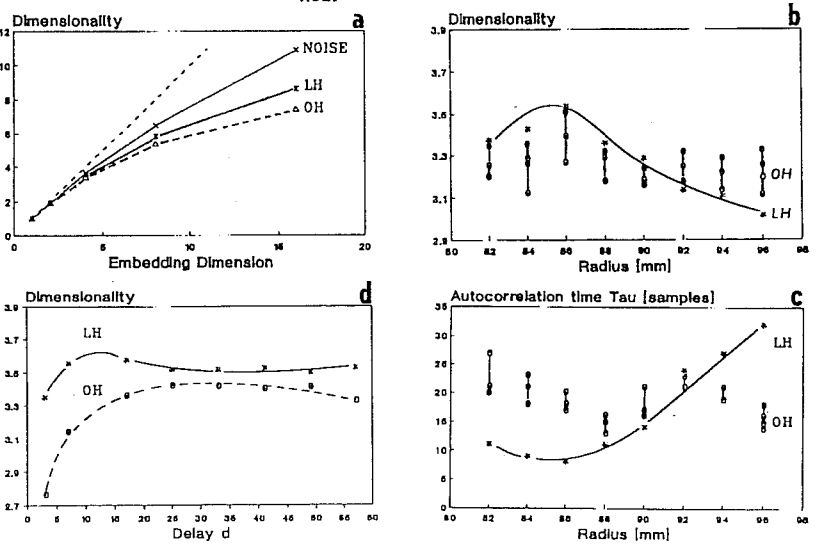

Fig.6. Dimensional and correlation analysis of density fluctuations